

RESEARCH

Open Access



Using skin biopsies to measure target occupancy of anti-fibrotic molecules: assay development and application for zampilimab in a primate model of chronic kidney disease and in healthy human volunteers

Linghong Huang^{1,4†}, Rowann Bowcutt^{1*†}, Alison Bigley², Graham Ogg³, Tim Schmidt^{1,5}, Geoffrey I. Johnston¹ and Timothy S. Johnson^{1,4}

Abstract

Background Assessing target engagement (TE) and target occupancy (TO) of novel antifibrotic molecules is challenging, as the target organs are inaccessible. In clinical trials, this often requires biopsies of internal organs, which increases both risk and discomfort for participants. Zampilimab (UCB7858) is a humanized monoclonal antibody that specifically inhibits the extracellular activity of transglutaminase 2 (TG2). Blocking TG2 activity reduces fibrosis in experimental models of chronic kidney disease. Here, a low-risk skin 'biopsy-on-biopsy' approach has been developed as a surrogate to assess TO of zampilimab in the kidney, ahead of further investigation of zampilimab in clinical studies.

Methods A dual-antibody competitive immunofluorescence assay was developed to assess TO of TG2 with zampilimab. A cynomolgus monkey unilateral ureteral obstruction model was used to assess zampilimab TO in the kidney and compare this with TE measured by an in situ TG activity assay. Data were compared with TO in dermal wounds in the same animals. A human skin 'biopsy-on-biopsy' dermal wound approach was developed to induce fibrosis-relevant pathways. Skin sections from healthy volunteers were incubated ex vivo with increasing doses of zampilimab to assess TO.

Results Zampilimab TO in cynomolgus monkey kidney and skin were positively correlated using our immunofluorescence assay, with an inverse correlation between skin TO and kidney TE using our in situ TG activity

[†]Linghong Huang and Rowann Bowcutt contributed equally to this work.

Alison Bigley and Geoffrey I. Johnston have since retired from their places of employment.

*Correspondence:
Rowann Bowcutt
rowann.bowcutt@ucb.com

Full list of author information is available at the end of the article



assay. In the human dermal wound model, maximal TG2 staining was observed on days 4–6 post initial dermal wound (biopsy). TO measurements increased dose-dependently with zampilimab application.

Conclusions Zampilimab inhibited TG2 in cynomolgus monkey kidney and skin. Skin is an accessible surrogate tissue to assess kidney TO and predict TE, and our ex vivo model of skin biopsy has potential for application in the development of other antifibrotic therapeutics. A phase I first-in-human study of zampilimab in healthy volunteers (NCT02879877; 26/08/2016) will provide further proof of concept.

Keywords Zampilimab, TG2, Fibrosis, Target occupancy, Target engagement, Biopsy-on-biopsy, Dermal wound model

Background

When developing novel therapeutics, defining the optimal dose of drug required to bind to its mechanistic target (target occupancy [TO]) to affect a measurable distal event (target engagement [TE]) is essential for calculating potential dosages and drug efficacy [1, 2]. However, assessing TO and TE poses challenges for therapies targeting organ fibrosis, as it is unethical to take internal organ biopsies from healthy volunteers [3]. Clinical endpoints for chronic fibrotic conditions can also take several years to be reached, which, in the absence of suitable surrogate markers, can impede clinical trials [4]. Validation of surrogate markers of TO and TE in target organs could therefore facilitate both healthy volunteer and clinical studies.

Transglutaminases (TGs) are a family of catalytically active enzymes that post-translationally modify proteins via deamidation and amine incorporation [5]. The TGs are involved in protein crosslinking, act as scaffolds, help to maintain structural integrity of membranes, regulate cell adhesion, and modulate signal transduction [5]. TG2 is a calcium-dependent enzyme widely distributed in cells and tissues but is one of only two TGs released into the extracellular matrix (ECM), where its crosslinking role enhances matrix stability and wound healing [5–7]. In addition to this crosslinking activity, TG2 is also involved in inflammation, cell growth, differentiation, and cell death [7].

Increased synthesis and extracellular trafficking of TG2 are associated with fibrosis and tissue scarring via both enzymatic and non-enzymatic mechanisms [8–10] in various tissues, including the heart [11], kidney [12], liver [13], and lung [14, 15]. Elevated levels of extracellular TG2 can lead to accelerated ECM deposition and reduced clearance, which underlies tissue scarring and fibrosis. Extracellularly, TG2 can crosslink ECM proteins with the formation of a stable, proteolytic resistant ϵ -(γ -glutamyl)-lysine isopeptide bond [16]. In addition to this direct stabilization of the ECM, TG2 also appears to indirectly promote ECM crosslinking via activation of the fibrotic cytokine transforming growth factor β (TGF- β) [17, 18].

The crucial role of TG2 in ECM remodeling and stabilization, which is involved in the development of fibrotic conditions, makes it an attractive therapeutic target. In chronic kidney disease (CKD), levels of TG2 are correlated with disease stage, and progressive disease is associated with high levels of TG2 in renal biopsy tissue and urine [12, 19, 20]. In rodent models of CKD, pharmacologic inhibition of TG2 activity leads to reduced fibrosis and preservation of kidney function [6, 21], while TG2 knockout mice are protected against the development of fibrotic lesions [22]. Additionally, in response to bleomycin-induced pulmonary fibrosis, TG2 knockout mice demonstrated reduced fibrosis [14, 23].

Zampilimab is an engineered, humanized, full-length monoclonal immunoglobulin G (IgG)4P antibody with a high affinity for human TG2 that specifically blocks the extracellular enzymatic function of TG2 by binding to an epitope in its core [24]. Zampilimab is in development for the treatment of fibrotic disease.

It is well reported that fibrosis is a type of unresolving, aberrant wound healing; thus, many mechanisms in fibrosis are synonymous with natural wound healing. In line with this, increased TG2 has been demonstrated in wounded skin in rats, with peak expression observed three days after the skin was wounded [25], consistent with initial work by Bowness et al., which demonstrated that TG activity increased in skin wound healing in rats [26]. Furthermore, TG2 expression and TO were demonstrated in an in vivo cynomolgus model of CKD, where TG2 was upregulated in wounded skin and TO in the skin of animals dosed with zampilimab was observed [27]. Additionally, in this model, fibrosis assessments (using high-content image analysis of Mason's trichrome-stained kidney tissue sections) showed that zampilimab reduced the fibrosis index by 16% at 10 mg/kg and by 81% at 50 mg/kg. These findings were confirmed by manual scoring of fibrosis in the tissue sections, which showed reductions of 35% and 42% in pathology scores, respectively [27]. This led to the hypothesis that creating a wound in human skin would lead to TG2 upregulation, and that by analyzing a biopsy from the wound site, TG2 expression could be measured to evaluate whether zampilimab binds to TG2 in vivo and subsequently inhibits its

activity. Thus, it may be possible to develop an approach using wounded skin for the ex vivo assessment of fibrotic processes, potentially serving as an accessible surrogate for fibrotic processes in internal organs, such as the kidney. In addition, we hypothesized that an immunofluorescent competition assay could be used to assess both the total TG2 present (antibody to non-therapeutic epitope) and the TO of zampilimab in vivo (using pre-labeled zampilimab binding to epitopes that were still available). This approach was considered applicable to both cynomolgus monkey and humans, given that TG2 proteins are highly conserved between the two species (see Fig. S1 in Additional file 1).

Here, we describe the application of this assay in kidney tissue from a unilateral ureteral obstruction (UVO) model of CKD and in wounded skin tissue from cynomolgus monkeys, to assess alignment between TO in the kidney and in the skin. We also compare TO with TE in the cynomolgus monkey CKD model using a substrate incorporation (in situ TG activity) assay. Finally, we describe optimization of the competitive binding assay for human use in a skin biopsy study (a research collaboration with the University of Oxford) and demonstrate its suitability for application in a phase I first-in-human study of zampilimab in healthy volunteers.

Methods

Animal work was completed by Prisys Biotechnologies (Shanghai, China) and approved by the Institutional Animal Care and Use Committee under study number 2015-PS11-002 (license code No. 204 0000037). Animals used in this study were purchased by Prisys Biotechnologies (Shanghai, China) from Hainan Jingang Biotech Co. Ltd., and housed in the animal vivarium at Prisys Biotechnologies. All materials were purchased from Sigma-Aldrich, Dorset, UK, unless otherwise stated.

Table 1 Zampilimab TO and TE assessment in cynomolgus monkeys in the preclinical model

Group	Operation	Treatment	Administration	Number of animals
1	Sham	Formulation buffer	Once weekly, for 4 weeks	2
2	None	Zampilimab 100 mg/kg	Once weekly, for 4 weeks	2
3	UVO	Formulation buffer	Once weekly, for 4 weeks	6
4	UVO	Zampilimab 10 mg/kg	Once weekly, for 4 weeks	6
5	UVO	Zampilimab 50 mg/kg	Once weekly, for 4 weeks	4

All doses of zampilimab were administered as 2 mL/kg intravenous bolus injections over 1–2 min

Abbreviations: TE target engagement, TO target occupancy, UVO unilateral ureteral obstruction

Preclinical, non-human primate model

UVO causes urine backflow, which leads to interstitial inflammation, tubular cell injury or atrophy, and ultimately, tubulointerstitial fibrosis. UVO replicates some of the features of obstructive kidney disease in humans and is a widely used model for CKD. A non-human primate UVO model developed and validated previously in cynomolgus monkeys [28] was used to assess zampilimab TO and TE in the fibrotic kidney.

Twenty healthy male cynomolgus monkeys aged 6–8 years were randomized using a simple randomization method to five groups for a prophylactic treatment study with post-surgery doses of zampilimab, high enough to give partial and complete blockade of activity (Table 1). Study personnel responsible for dosing were aware of the experimental groups during the dose allocation and throughout the study. Scientists responsible for running assays and those involved in data analysis were blinded to the experimental groups until all analyses had been performed.

Each monkey was housed in one stainless-steel cage (minimum living area of 160 × 80 × 190 cm), maintained at a temperature of 18–29 °C and a relative humidity of 40–70%. Animal rooms were enriched with natural light through glass windows and cages were enriched with mirrors and balls. Animals also had access to the exercise cage (480 × 80 × 190 cm) with enrichment devices for 24 h every week. Monkeys had free access to monkey chow (Guangzhou Guolong Science & Technology Co. Ltd., China) and municipal tap water that met human drinking water standards. In addition, monkeys received regular vegetable and fruit treats.

The monkeys were screened prior to selection for any signs of existing CKD; only animals with a serum creatinine ≤ 125 μmol/L and urine albumin creatinine ratio < 2.5 were included in the study. Before surgery, monkeys were sedated and immobilized by intramuscular injection of tiletamine and zolazepam (Zoletil™ 50; 5 mg/kg) and were anesthetized by isoflurane inhalation (5% for induction; 2% for maintenance). Lornoxicam was administered (IV 0.7 mg/kg) 20 min before the surgery and oral codeine was dosed (0.5 mg/kg) 2 h prior to surgery. Monkeys in groups 3–5 (Table 1) underwent surgery to induce UVO, where the left ureter was dissected and ligated at two points using a silk tie, as previously described [28]. Group 1 (sham) animals received the same surgery, excluding the ureter ligation, and group 2 animals had no intervention. After surgery, monkeys received penicillin (25,000 IU/kg, twice daily) and lornoxicam (0.35 mg/kg, twice daily) for 3 days, and codeine was given orally (0.5 mg/kg, three times a day) for 2 days.

Post surgery, varying doses of zampilimab were administered intravenously over 4 consecutive weeks, as shown in Table 1. Animals were observed daily during the study

period for signs of illness and general health/reaction to treatments. At study termination, animals were sacrificed by phenobarbital overdose. The left UO and right contralateral kidneys were removed, halved longitudinally, and each half was cut radially from the papilla into four segments. Segments were snap frozen and cryosections were prepared for analysis. Monkey kidney was assessed to determine zampilimab TO and TE using the competitive immunofluorescence assay and *in situ* TG activity assay, respectively. Skin tissue was harvested from the UO formulation buffer and the 10 mg/kg and 50 mg/kg zampilimab groups. At study termination, 3×1 cm skin sheets were harvested from each animal and snap frozen in liquid nitrogen for preparation of cryosections. Monkey skin TO was measured using the competitive immunofluorescence assay to determine any correlation between kidney TO and TE in the UO model.

Blood samples were collected before UO surgery, at regular intervals during the study, and at study termination. Levels of circulating zampilimab were assessed in plasma samples by liquid chromatography-electrospray ionization with tandem mass spectrometry. This method had a limit of quantification of 1 µg/mL for zampilimab.

The protocol was registered with Prisys Biotechnologies (Shanghai, China), who conducted the study in accordance with the protocol and the standard operating procedures. Animal work was completed by Prisys Biotechnologies and approved by the Institutional Animal Care and Use Committee under study number 2015-PS11-002 (license code No.204 0000037). UCB representatives (including an animal care and welfare officer) assessed facilities and procedures prior to the study start to ensure best practice animal welfare in accordance with United Kingdom (UK) Home Office guidelines and the Animal Scientific Procedures Act 1986 (ASPL). A UCB representative was present during all animal experiments to ensure compliance with ASPL.

Competitive immunofluorescence assay

To simultaneously identify both TG2 and zampilimab for the assessment of TO, an assay using fluorescently-labeled zampilimab and fluorescently-labeled anti-TG2 antibodies, with binding epitopes remote from the zampilimab binding site (in-house monoclonal antibodies [mAbs] IA12 and DH2), was developed.

Frozen 6 µm kidney or skin sections were air dried for 5 min, rinsed with phosphate buffered saline (PBS), and incubated for 30 min in blocking buffer (PBS with 5% bovine serum albumin [BSA] and protease inhibitors). Sections were incubated with 30 µg/mL of an Alexa Fluor® 546-labeled zampilimab and an Alexa Fluor® 488-labeled TG2 antibody (IA12 or DH2) for 1 h at 37 °C. PBS-Tween was used to wash the sections, followed by a final 5 min wash in PBS before the sections were fixed in ice cold acetone

and air dried, then washed and mounted using VectaShield hard-set mounting media containing 4',6-diamidino-2-phenylindole (DAPI). Images were analyzed by OracleBio (Biocity, UK) on a Visiopharm platform (Hoersholm, Denmark) to compare the relative binding of red pixels (Alexa Fluor® 546-labeled zampilimab, which is competitively inhibited by unlabeled zampilimab administered *in vivo*) to green pixels (anti-TG2 antibodies revealed with Alexa Fluor® 488 secondary antibody) to calculate percentage TO (Fig. 1A). To quantify TO, image analysis was used to calculate the area stained green (representing 'total' TG2 binding as revealed by Alexa Fluor® 488-labeled DH2/IA12) and the area that appears yellow on merged images (representing co-localized staining by Alexa Fluor® 488-labeled DH2/IA12 and Alexa Fluor® 546-labeled zampilimab, binding at different TG2 epitopes). The difference between the green area and yellow area represents the area in which competitive binding prevented Alexa Fluor® 546-labeled zampilimab from binding, which can be calculated as a proportion of total TG2 binding (green area) to provide a value for percentage TO. TG2 staining with IA12 and DH2 antibodies was compared in cynomolgus monkey skin sections.

In situ TG activity assay

Unfixed, frozen, 6 µm kidney sections were washed in PBS twice and incubated for 30 min at room temperature in reconstitution buffer (1% BSA and 5 µg/mL streptavidin to prevent non-specific binding) with protease inhibitors (1.04 mM 4-[2-aminoethyl benzenesulfonyl] fluoride [AEBSE], 0.8 µM aprotinin, 40 µM bestatin, 14 µM E-64, 20 µM leupeptin, and 15 µM pepstatin A). Sections were washed twice in PBS then incubated with reaction mix (5 mmol/L CaCl₂, 1 mmol/L 1,4-dithiothreitol, 0.5 mmol/L biotinylated cadaverine with protease inhibitors) for 1 h at 37 °C, then washed three times in PBS and fixed in ice cold acetone for 5 min. For the negative control samples 10 mmol/L ethylenediaminetetraacetic acid (EDTA) was used in place of CaCl₂. After air drying, sections were washed in PBS and blocked (5% BSA in PBS) for 30 min at room temperature and incubated with a 1 in 500 dilution of streptavidin-Alexa Fluor® 555 for 1 h at 37 °C. Sections were then washed three times in PBS and mounted in antifade mounting media containing DAPI. The area of incorporated biotin cadaverine visualized by streptavidin Alexa Fluor® 555 binding was quantified by image analysis, performed by OracleBio using a Visiopharm platform, to provide an estimate of TG activity.

Statistical analysis

The Spearman rank correlation coefficient was used to evaluate the relationship between: kidney TO and skin TO, kidney TO and kidney TG activity, kidney TG activity and skin TO, kidney TO and circulating zampilimab, kidney TG activity and circulating zampilimab, and

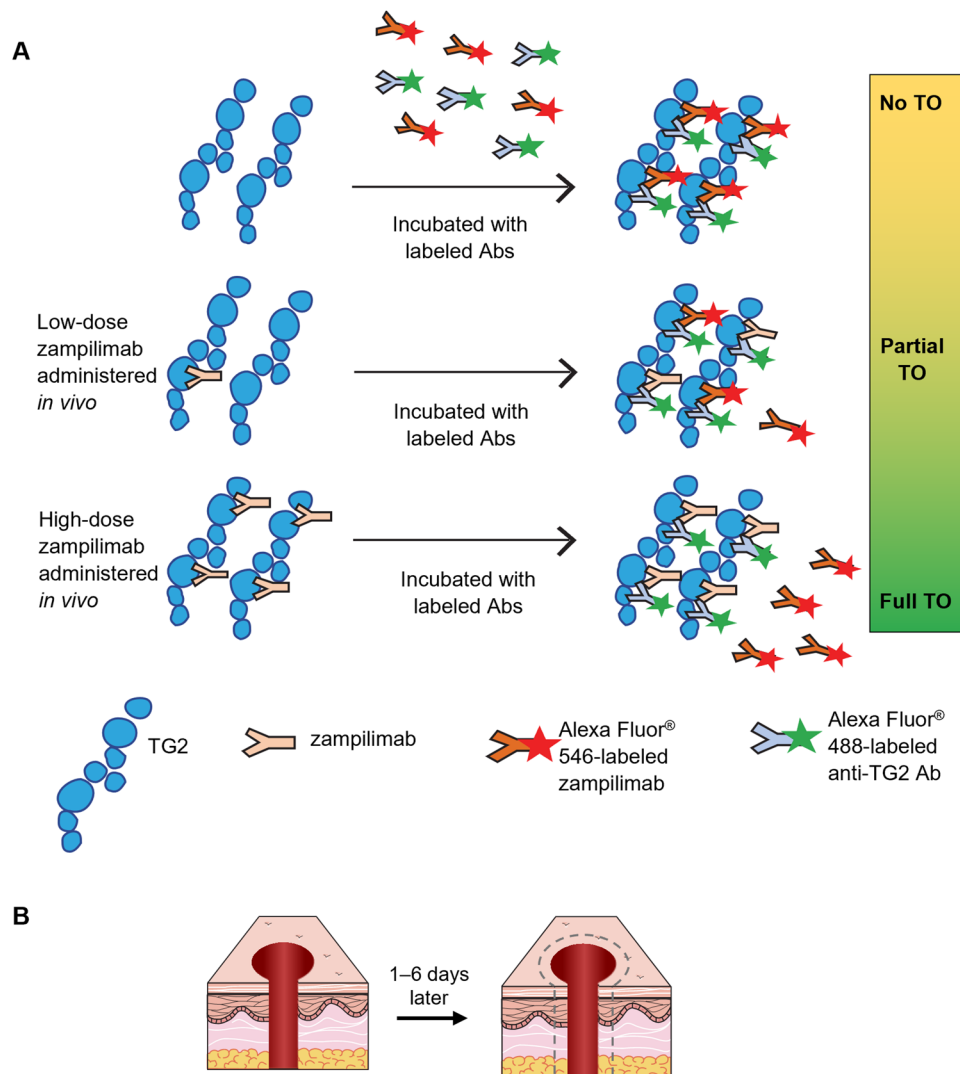


Fig. 1 Assessing zampilimab TO in skin. **(A)** Alexa Fluor[®] 546-labeled zampilimab antibody (Ab; red star) and Alexa Fluor[®] 488-labeled anti-TG2 Ab binding a distant epitope (green star) were used. TO was measured by comparing the relative binding of Alexa Fluor[®] 546 (competitively inhibited by unlabeled zampilimab administered *in vivo*) to Alexa Fluor[®] 488. 'No TO' is shown as yellow, with both labeled antibodies binding equally. 'Full TO' is shown with Alexa Fluor[®] 488 (green), as Alexa Fluor[®] 546-labeled zampilimab binding is prevented following zampilimab administration. **(B)** 3 mm punch biopsy was taken from the buttock and closed with a suture. This was punched out with a 6 mm punch 1 to 6 days later and the biopsy was frozen and sectioned for staining. Abbreviations: Ab antibody, TG2 transglutaminase 2, TO target occupancy. Skin image adapted from: Server Medical Art. Available at: https://smart_image/burns/. With permission © 2020 (<https://creativecommons.org/licenses/by/3.0/>)

skin TO and circulating zampilimab. Individuals were removed from the analysis if no blood vessels were visible in the samples obtained.

Human skin biopsy study

The study was a research collaboration with the University of Oxford and was approved by the South Central - Oxford B Research Ethics Committee (reference 16/SC/0457), in accordance with the Declaration of Helsinki.

Skin biopsies were obtained from sun-protected sites on 12 adult healthy volunteers recruited at University of Oxford University Hospitals, UK. A 3 mm punch biopsy was performed in the buttock and closed with a

suture; the skin wound was then excised with a subsequent 6 mm punch 1–6 days later (varying intervals were used to permit assessment of chronological changes in skin TG2 post injury; Fig. 1B). The term 'biopsy on biopsy' was used to describe this approach of using the initial biopsy to upregulate wound response proteins in the skin. Sections of wounded skin were incubated for 30 min *ex vivo* with increasing concentrations of zampilimab (0.0001–2 µg/mL) and washed extensively. As for the non-human primate skin model, TO of zampilimab was assessed in dermal wound skin using the competitive immunofluorescence assay. To mimic the different levels of TO from *in vivo* studies, labeled zampilimab

and labeled TG2 antibody targeting a remote epitope (DH1/IA12) were incubated on the sections at the same time. We assessed any potential steric hinderance and found <20% difference between single and co-administration. The maximum co-localization signal and minimum Alexa Fluor® 488 and Alexa Fluor® 546 only signals were observed at 28.5 ms and 56.9 ms exposure times, respectively (Hamamatsu Nanoscope, Model C9600-12, Olympus, Japan; filter sets used: DAPI, fluorescein isothiocyanate, tetramethyl rhodamine iso-thiocyanate).

Results

Preclinical proof of concept in a non-human primate model of CKD

TG2 staining with IA12 and DH2 antibodies was compared in cynomolgus monkey skin sections. Although stained structures were similar, blood vessels stained

with DH2 had stronger signal intensity and better resolution than those stained with IA12 (Fig. 2) DH2-labeled with Alexa Fluor® 488 was therefore selected as the TG2 antibody to measure the total TG2 in the TO assay in cynomolgus monkey kidney and skin tissues.

Kidney and skin sections from untreated UUO monkeys were stained with Alexa Fluor® 546-labeled zampilimab and Alexa Fluor® 488-labeled DH2. Both antibodies demonstrated clear and strong TG2 antigen staining (Fig. 3 [column 1; kidney and column 4; skin]), with excellent co-localization. The location of staining in the kidney was consistent with that previously reported [12], while staining in the skin was most intense in and around blood vessels. Kidney staining was also consistent with a prior study assessing TG activity measured using a biotinylated cadaverine in situ TG activity assay [28].

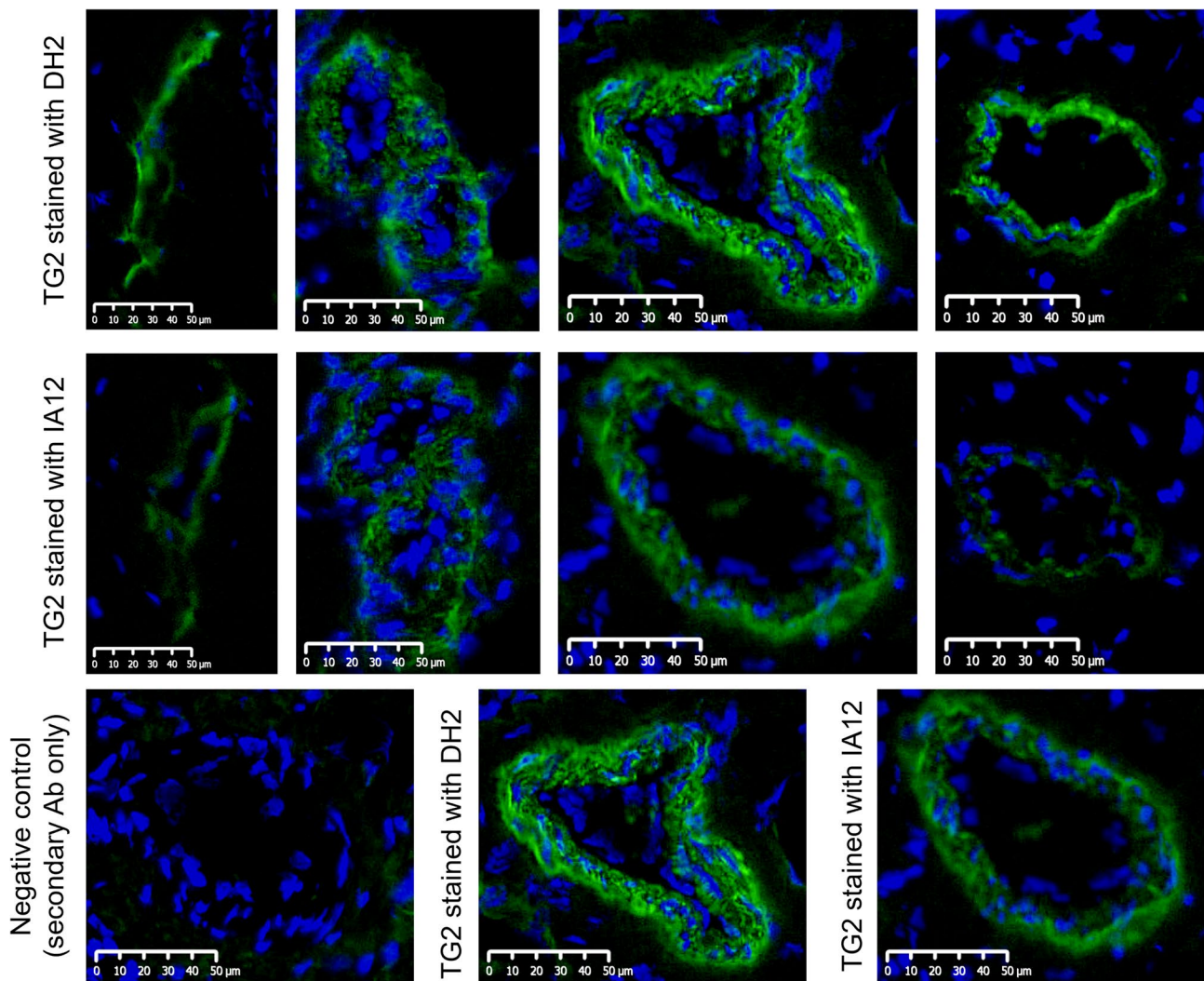


Fig. 2 TG2 staining in cynomolgus monkey skin sections using anti-TG2 antibodies. TG2 staining using Alexa Fluor® 488-labeled DH2 and Alexa Fluor® 488-labeled IA12 anti-TG2 antibodies (green) with DAPI nuclei (blue) is localized mainly to blood vessels within the dermis and was stronger with DH2 than IA12. Abbreviations: Ab antibody, DAPI 4',6-diamidino-2-phenylindole, TG2 transglutaminase 2

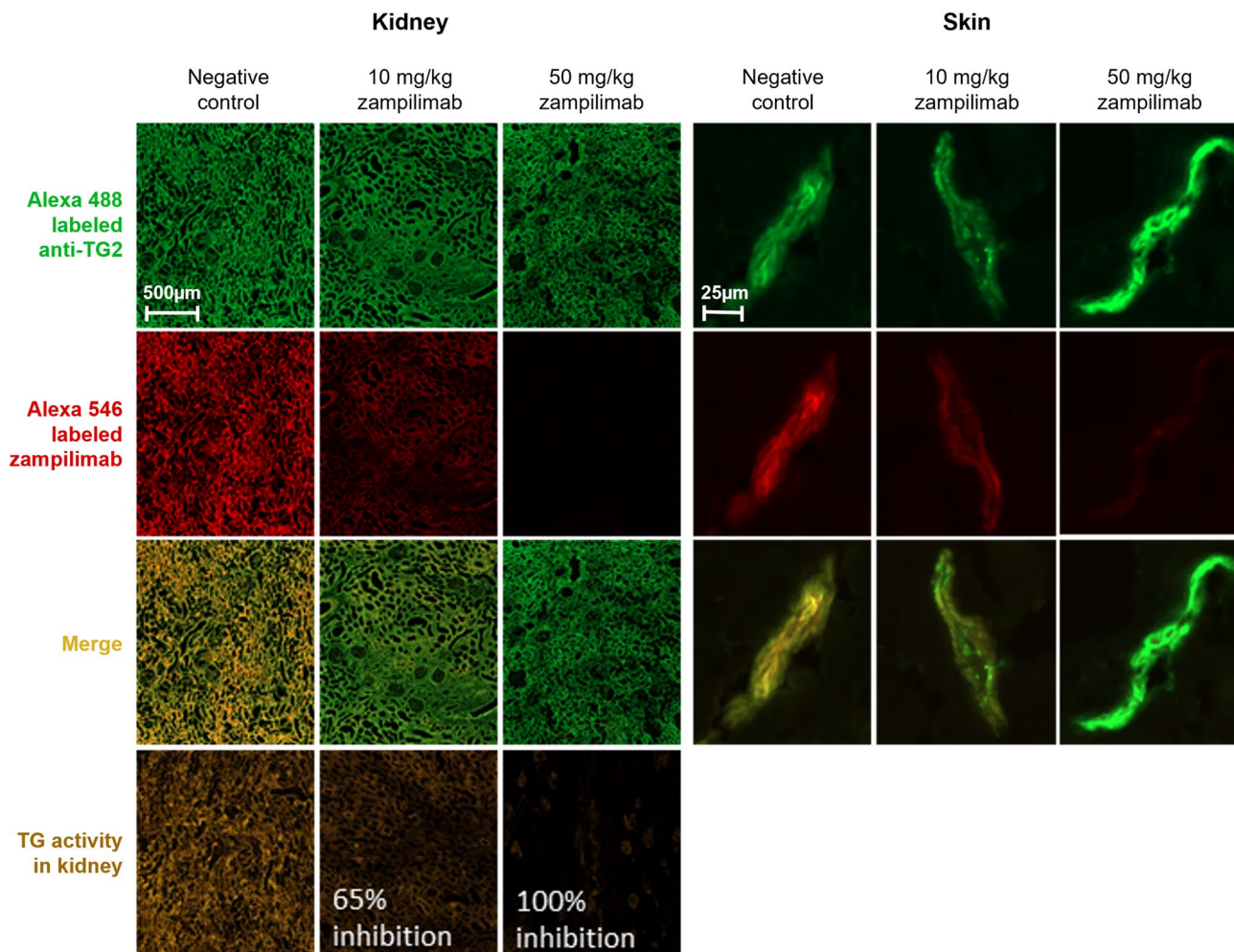


Fig. 3 TG2 staining in cynomolgus monkey kidney (UUO model of CKD) and skin sections. Alexa Fluor® 488-labeled anti-TG2 antibody (DH2) indicates the presence of TG2 in the kidney and skin (row 1). Binding of Alexa Fluor® 546-labeled zampilimab is competitively inhibited by zampilimab pre-treatment in vivo (row 2). Merged images (row 3) reveal the difference between total TG2 and Alexa Fluor® 546-labeled zampilimab binding to provide a measure of TO. TG activity in the kidney decreased with zampilimab pre-treatment at increasing dosages (row 4) consistent with the reduction in Alexa Fluor® 546-labeled zampilimab staining (row 2). *Abbreviations:* CKD chronic kidney disease, TG transglutaminase, TO target occupancy, UUO unilateral ureteral obstruction

In kidney and skin sections from UUO monkeys treated with zampilimab 10 or 50 mg/kg for 4 weeks, Alexa Fluor® 488-labeled DH2 staining was comparable to that in control (untreated) cynomolgus monkey tissue (Fig. 3 [row 1; green staining]). In contrast, Alexa Fluor® 546-labeled zampilimab staining was reduced with increasing doses of zampilimab applied in vivo (Fig. 3 [row 2, columns 2, 3, 5, and 6; red staining]). These data demonstrate competitive inhibition of Alexa Fluor® 546-labeled zampilimab binding, i.e., occupancy of the TG2 zampilimab binding site, following intravenous administration of zampilimab in vivo. This image analysis confirmed dose-related reduction in Alexa Fluor® 546-labeled zampilimab staining which equates to increases in calculated TO in both kidney and skin tissue, following intravenous zampilimab administration (Fig. 4A, B).

The TG in situ activity assay showed 65% and 100% reductions in TG activity in the kidney following in vivo administration of zampilimab 10 mg/kg or 50 mg/kg, respectively (Fig. 3 [row 4]; Fig. 4C), indicating dose-related inhibition of TG by zampilimab in vivo (i.e., TE). This was consistent with the reduction in Alexa Fluor® 546-labeled zampilimab staining (Fig. 3 [row 2]).

A series of correlation analyses were conducted to explore relationships between TO in kidney and skin, and TO and TG activity in the kidney (Fig. 4D–F). Positive correlation between TO in kidney and TO in skin was observed ($r=0.72$, $p=0.0106$; Fig. 4D). TO and TG activity in kidney were highly inversely correlated ($r=-0.75$, $p<0.01$; Fig. 4E), and there was also an inverse correlation between skin TO and TG activity in kidney ($r=-0.78$, $p=0.0017$; Fig. 4F). Kidney and skin TO, and

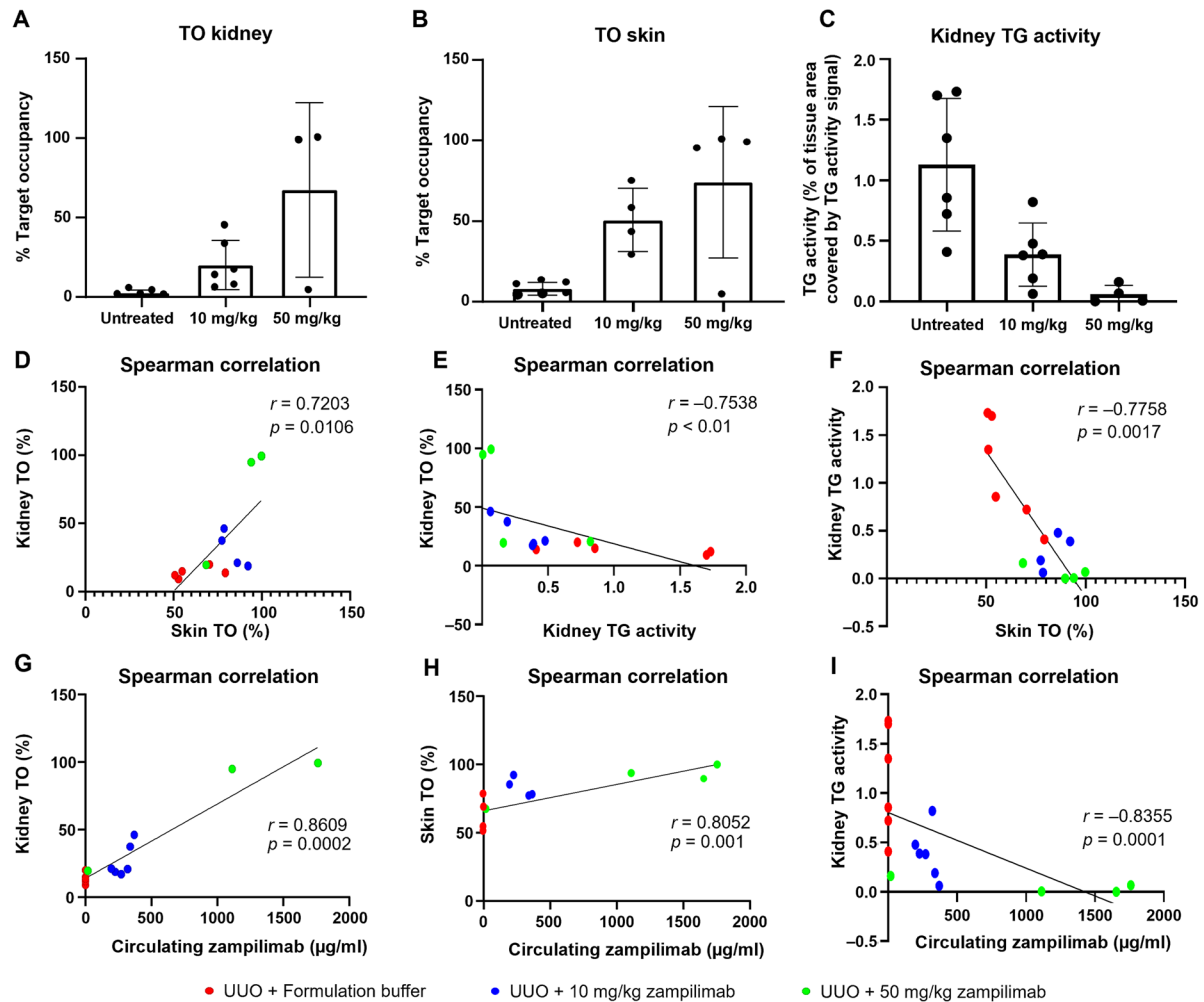


Fig. 4 TO of zampilimab and TG activity in the cynomolgus monkey UUO model. Kidney TG activity is measured as percentage tissue area covered by TG2 signal (C, E, F and I). There is an inverse correlation between TO and TG activity (TG activity decreases as TE or TO increases). TO increased with increasing zampilimab dose in kidney (A) and skin (B). TG activity in the kidney decreased with increasing zampilimab dose (C) indicating increasing TE. TO in the kidney correlated with TO in the skin (D). TO in kidney and skin were correlated with TE in the kidney (E, F). Circulating levels of zampilimab correlated positively with kidney and skin TO (G, H) and negatively with TE (I). Mean and standard deviation are plotted in A–C. Missing data points for kidney TO (A, D, E, and G; animal receiving 50 mg/kg zampilimab and untreated UUO animals) are due to exhausted samples. Data points for skin TO (B, D, and H; animals receiving treated with 10 mg/kg zampilimab) were excluded from the analysis as no blood vessels were visible in the samples. Different colour thresholds to define signals were used to determine TO in the skin (B and F); the trend of change is similar across both assessments. The high level of TO observed in untreated animals (D and F) is due to increased background (autofluorescence) being detected as a signal in some of these data. Abbreviations: TE target engagement, TG2 transglutaminase 2, TO target occupancy, UUO unilateral ureteral obstruction

kidney TG activity were also correlated with the levels of circulating zampilimab (kidney TO: $r = 0.86$, $p = 0.0002$ [Fig. 4G]; skin TO: $r = 0.81$, $p = 0.001$ [Fig. 4H]; kidney TG activity: $r = -0.83$, $p = 0.0001$ [Fig. 4I]).

Human skin biopsy study

Having obtained proof of concept that an immunofluorescent antibody competition assay in skin could mirror both TO and TE in the kidney in a non-human primate model, applicability of the assay to human skin was established. Preliminary work in human skin aimed

to determine the best timepoint for evaluation of zampilimab TO in the human dermal wound model. We explored chronological changes in skin TG2 post injury in recovery punch biopsies taken at different intervals 1–6 days after the initial punch biopsy insult. Immunofluorescence staining of sections from the 6 mm punch biopsies with IA12 and zampilimab showed that TG2 expression was detectable by 24-h post wounding and remained elevated over the 6 days (Fig. 5A). The expression of TG2 was mainly localized to blood vessels. Quantification using high-content image analysis showed that

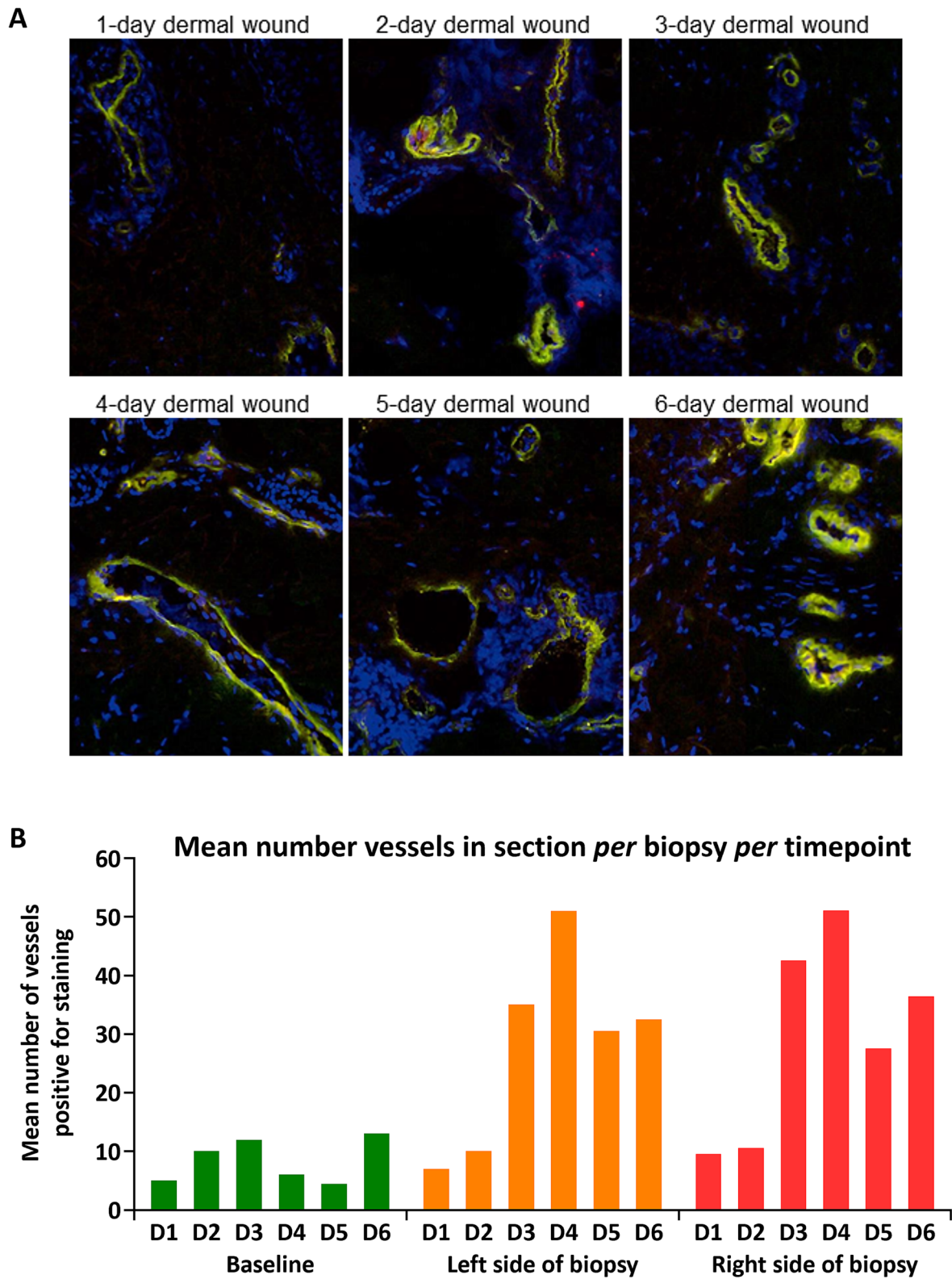


Fig. 5 Target occupancy assay performed in untreated human dermal wound. Wounded dermal skin samples from healthy volunteers taken at different time points were sectioned. Cryostat sections were stained with Alexa Fluor® 546-labeled zampolimab (red) and Alexa Fluor® 488-labeled IA12 (green). **A** Images of the combined staining are shown as yellow. **B** Quantification of number of vessels positive for staining. *Abbreviations:* D day

the number of TG2-positive vessels reached a maximum at day 4 post wounding, but TG2 staining was sufficiently high for robust analysis over days 3–6 (Fig. 5B).

To establish the best exposure times for co-localization of the two antibodies, and thus TO, evaluations were made at a range of different exposure combinations (Fig. 6). Overall, there was little difference between the performance of IA12 and DH2, with exposure combination 3 (Alexa Fluor® 488-labeled IA12/DH2: 28.5 ms, Alexa Fluor® 546-labeled zampilimab: 56.9 ms) providing the best co-localization characteristics for both antibodies, and longer exposures potentially resulting in autofluorescence in the red channel. Both Alexa Fluor® 488-labeled IA12 and DH2 appeared to be suitable partner antibodies to assess total TG2 with good co-localization and exposure characteristics.

Subsequent work aimed to assess trends in co-localization of TG2 and zampilimab, using two in-house TG2 antibodies, DH2 or IA12, and Alexa Fluor® 546-labeled zampilimab. Biopsies taken from healthy volunteers on day 4 post wounding were used for ex vivo pre-application of a dilution series of unlabeled zampilimab (0.0001–2 µg/mL) for 1 h. After this time, sections were washed and the TO immunofluorescent antibody competition assay was carried out. TO of zampilimab was demonstrated by the dose-dependent, secondary prevention of Alexa Fluor® 546-labeled zampilimab binding (Fig. 7). Both Alexa Fluor® 488-labeled IA12 (Fig. 7A) and DH2 (Fig. 7B) co-localized strongly with zampilimab in

wounded skin. In addition, high levels of co-localization were observed when preincubation with unlabeled zampilimab did not occur. In sections preincubated with zampilimab, Alexa Fluor® 488-labeled IA12 and DH2 binding was maintained. However, zampilimab binding was progressively reduced as the concentration of preincubation zampilimab increased, with a lower level of co-localization in the merged image (Fig. 7). Although preincubation with high-dose zampilimab (1.5 µg/mL) had no effect on Alexa Fluor® 488-labeled IA12 or DH2 binding, no Alexa Fluor® 546-labeled zampilimab staining was evident, and the merged image remained bright green (Fig. 7). Staining patterns with Alexa Fluor® 488-labeled IA12 and DH2 were similar to that of the cynomolgus monkey tissues, with Alexa Fluor® 488-labeled DH2 providing higher intensity staining (Fig. 7).

High-content image analysis demonstrated a classical dose-response curve when zampilimab TO (co-localization) was determined using either Alexa Fluor® 488-labeled DH2 or IA12 total TG2 reference antibodies (Fig. 8). However, the zampilimab dose-response curve characteristics differed when using these two antibodies. Alexa Fluor® 488-labeled IA12 remained at 80–85% co-localization up to 0.01 µg/mL of pre-incubated zampilimab, dropped to zero between 0.01 and 1 µg/mL, and remained at zero at higher doses, suggesting that this assay had a 100-fold working range. Alexa Fluor® 488-labeled DH2 had a lower co-localization when no preincubation occurred, with a progressive drop at

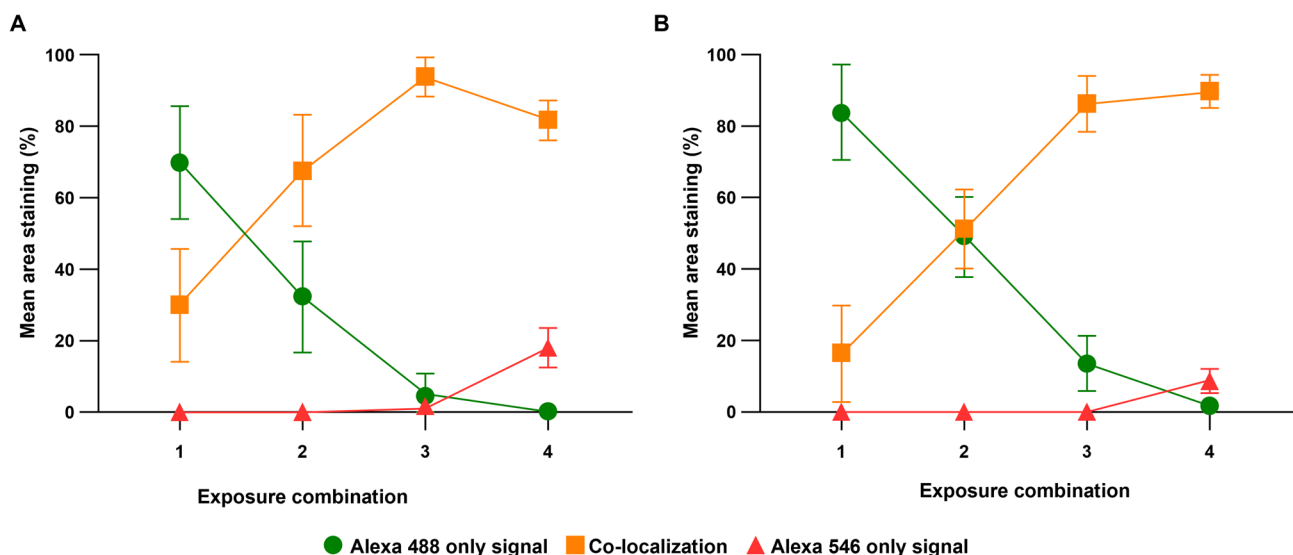


Fig. 6 Quantification of co-localization of zampilimab and IA12 or DH2 over a range of exposures. From exposure combinations 1 (Alexa Fluor® 488-labeled IA12/DH2: 28.5 ms, Alexa Fluor® 546-labeled zampilimab: 14.2 ms), 2 (Alexa Fluor® 488-labeled IA12/DH2: 28.5 ms, Alexa Fluor® 546-labeled zampilimab: 28.5 ms), 3 (Alexa Fluor® 488-labeled IA12/DH2: 28.5 ms, Alexa Fluor® 546-labeled zampilimab: 56.9 ms) and 4 (Alexa Fluor® 488-labeled IA12/DH2: 28.5 ms, Alexa Fluor® 546-labeled zampilimab: 113.9 ms) for IA12 and DH2, there is a gradual reduction in Alexa Fluor® 488 only and a gradual increase in co-localization between IA12/DH2 and zampilimab. This demonstrates that the maximum area of co-localization of target and zampilimab is defined at Exposure 3. Alexa Fluor® 488-labeled IA12 and DH2 are both suitable partner antibodies to assess total TG2. Mean and standard deviation are reported for 3 participants. *Abbreviations:* ms milliseconds, TG2 transglutaminase 2

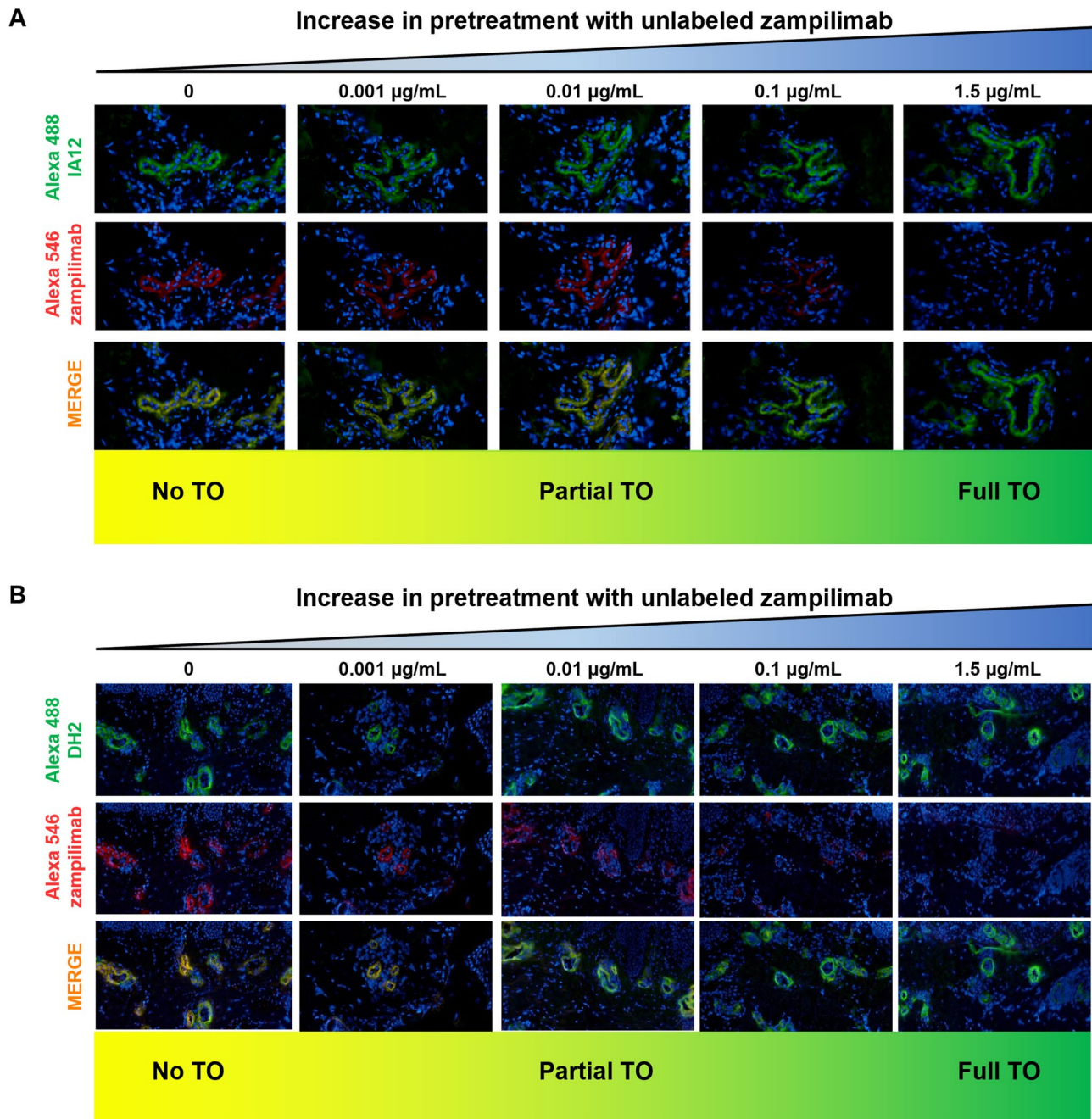


Fig. 7 Human skin biopsy study of zampilimab TO. Skin sections were pre-treated ex vivo with increasing doses of unlabeled zampilimab, and then incubated with Alexa Fluor® 488-labeled anti-TG2 antibodies IA12 (**A**) or DH2 (**B**) and Alexa Fluor® 546-labeled zampilimab. This demonstrated assay proof of concept in human tissue and identified IA12 as the preferred anti-TG2 antibody for use in the human tissue assay. DAPI nuclear staining is shown in blue. Abbreviations: DAPI 4',6-diamidino-2-phenylindole, TG2 transglutaminase 2, TO target occupancy

increasing zampilimab doses and near total loss of co-localization by 1.5 µg/mL. A persistent spike in percent co-localization was observed at 0.01 µg/mL of zampilimab. Alexa Fluor® 488-labeled DH2 therefore provided a wider and more dynamic range; however, interpretation and therefore IC₅₀ calculation are compromised by the non-linear response.

Discussion

One of the major challenges faced in developing novel anti-fibrotic therapies is establishing if the intended target has been manipulated early in clinical studies with the applied dose. Most fibrotic studies require extended treatment periods (at least 12 months) to alter disease markers, which can have both ethical and financial implications with regards to dosing. Additionally, many

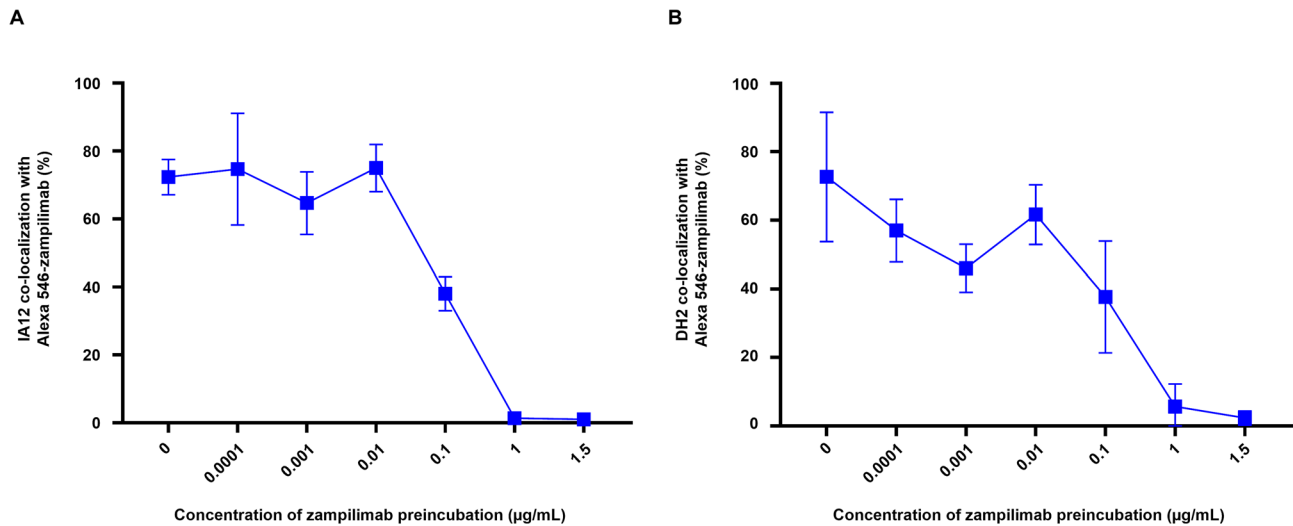


Fig. 8 Quantification of the percentage overlap of IA12 and DH2 at different concentrations of zampilimab preincubation. Frozen skin sections were preincubated with unlabeled zampilimab at various concentrations. Unlabeled zampilimab competes with Alexa Fluor® 546-labeled zampilimab so that the co-localization of Alexa Fluor® 488-labeled IA12 (**A**) or DH2 (**B**) and Alexa Fluor® 546-labeled zampilimab are inhibited. A concentration of 1 µg/mL unlabeled zampilimab completely inhibits Alexa Fluor® 488-labeled IA12/DH2 and Alexa Fluor® 546-labeled zampilimab co-localization. Area, percentage and TO trends were similar for both IA12 and DH2 across all preincubation concentrations, which is suggestive of a similar performance. These results show that either Alexa Fluor® 488-labeled IA12 or DH2 would be effective pairs for Alexa Fluor® 546-labeled zampilimab to assess total TG2 and TO. Mean and standard error are reported for 3 participants. *Abbreviations:* TG2 transglutaminase 2, TO target occupancy

fibrotic mechanisms are associated with normal physiology and excess dosing can lead to unnecessary toxicity. Furthermore, most fibrotic diseases affect internal organs. Sampling internal organs by biopsy carries risk, is unpleasant for the patient, and subsequently, this combination limits assessment of target manipulation for the duration of the treatment period. To address these challenges, we exploited the fact that fibrosis represents aberrant wound healing and that many of the pathways elevated in fibrosis are transiently elevated in normal wound repair. By inducing a low-risk and accessible dermal wound by biopsy and then recovering that dermal wound with a larger biopsy, we were able to determine the kinetics of TG2 upregulation post wounding, observing a peak in TG2 expression on day 4 post wounding. The detection of TG2 post wounding allowed us to use the ‘biopsy-on-biopsy’ wound method to evaluate TO without the highly invasive biopsy of an internal organ.

To provide proof of concept of this approach, we successfully developed a competitive immunofluorescence assay to accurately quantify TO of the TG2 inhibitory antibody zampilimab in the wounded skin of humans. In addition, we demonstrated correlation with both TO and TE in the kidney using a non-human primate model of kidney fibrosis. We hypothesized that applying labeled TG2-specific antibodies capable of recognising an epitope remote from zampilimab could be used to detect total TG2 (mAbs IA12 or DH2; AlexaFluor® 488; green-labeled) and bind to TG2 regardless of the amount of zampilimab available in the circulation or tissue. The

degree of directly labeled zampilimab (AlexaFluor® 546; red-labeled) that was able to bind would then be dependent on how much of the available TG2 had already been bound in vivo by unlabeled zampilimab (Fig. 1A). The combined colour (signal) following TG2 staining indicated the levels of TO in the tissue. Through image analysis, it was possible to quantify changes in binding and therefore changes in TO (Figs. 3 and 5).

The UUO cynomolgus monkey model of fibrosis in our study showed TO of zampilimab in the kidney, which was highly correlated to TO in the skin. Subsequently, correlation of TO to TE (assessed by TG activity) in the kidney using the in situ TG activity assay provided confidence that TO was linked to TE. Monkey kidney TO and TE and skin TO were also correlated with circulating levels of zampilimab. Replication of these results in the human skin biopsy study with ex vivo incubation of zampilimab provide proof of concept for the ‘biopsy-on-biopsy’ skin approach as a measure of zampilimab TO, which could be applied in clinical studies.

An alternative approach to developing the competitive immunofluorescence assay could have been to use the application of labeled zampilimab with reduced binding as an indication of increased TO. While this approach would be simpler, the amount of TG2 present in the biopsy would be unclear as a low level of labeled zampilimab binding could indicate TO or suggest sampling of a low TG2 area had occurred compared with a previous biopsy. A second antibody (to provide a benchmark) not only reduces this concern as it enables calculation of

TO as a percentage of available TG2 but allows a single biopsy to be used to evaluate TO as no reference to prior TG2 level is required. However, while beneficial, to prevent the two antibodies hindering one another, cooperative antibody pairs are needed. In this case, we knew from previous work where various antibodies would bind [24]; zampilimab binds to an epitope at amino acids 313–327 in the catalytic core, while DH2 and IA12 bind to amino acids 450–467 and 372–409 in the same core region, respectively [24]. Theoretically, as the epitopes are separate, IgG binding to one epitope should not be affected by the binding to another; however, IgG is large (150 kDa), and multi-labeled IgG is larger still, therefore, the risk of steric hindrance requires determining empirically. During optimization of the assay in human skin, while DH2 gave a slightly stronger signal, all other evaluations were comparable between IA12 and DH2. However, there was an unexpected and persistent spike at 0.01 µg/mL of zampilimab that could not be explained. Thus, to avoid complications in the interpretation of data, IA12 was selected as the antibody to pair with zampilimab due to the linear response in its working range, which was sufficient for incorporation into our phase I first-in-human study.

Skin contains multiple members of the TG family (TG1, TG3, and TG5) in addition to TG2, that have a conserved catalytic core [5] and that catalyze the same crosslinking reaction. While there are substrates for TG2, such as the Hitomi T26 peptide [29], these are not completely specific, but rather preferential substrates. Therefore, the large excess of TG1, 3, and 5 in skin means that *in situ* TG activity assays are not specific enough to assess TG2 activity in the skin.

These studies have some limitations. For the TO assay optimization for human skin, only one skin section was analyzed during antibody titrations; therefore, variances in vessel profiles and associated labeling may have affected overall outcomes. Additionally, in some samples, no blood vessels were visible, and some samples became exhausted, which led to individuals being excluded from analyses. The intensity levels of the fluorescent labeling were also lower than expected (compared with animal tissues), meaning that minor changes in intensity may have had an impact on the results. These limitations suggest that future studies should include at least three technical repeats and utilize at least three known controls to cover an identifiable range of TO and standard fluorescent signal detections.

Overall, the techniques described here provide useful tools to evaluate novel antifibrotic therapies in the clinic in the absence of other TO and TE options. We have shown that zampilimab successfully targets and engages TG2 in a non-human primate UUO model of CKD, with consistency between TO in the kidney and the skin, and we repeated these observations at wound sites in human skin biopsies to provide relevance to patient studies. Replication of these results in a subsequent

phase I first-in-human study in healthy volunteers (NCT02879877; 26/08/2016), with single ascending doses of zampilimab will provide proof of concept for the ‘biopsy-on-biopsy’ skin model (unpublished observations: Collier J, Bowcutt R, Johnston GI, Chan JYC, Raievska A, Bigley A, Nicholl R, Schmidt TS, Sarno M, Ali Z, Thomson E. Randomized phase I studies evaluating the safety, tolerability, pharmacokinetics, and target occupancy of zampilimab in healthy participants. In development). Together, these assays provide evidence that skin may be a surrogate organ to indirectly estimate the TO of novel therapeutics when measurement *in situ* is not possible. This method could be applied in both healthy-volunteer and early-patient studies, where surrogate biomarker assessments are not possible, and clinical outcomes can take years to assess [4].

Conclusion

In conclusion, we have developed and optimized a quantifiable, immunofluorescence-based assay that demonstrated skin is an accessible surrogate organ, to assess TO of novel antifibrotic therapeutics. Using this assay, we have shown that zampilimab can inhibit TG2 in a non-human primate UUO model and in human skin biopsies.

Abbreviations

Ab	Antibody
AESBF	4-(2-aminoethyl) benzenesulfonyl fluoride
ASPL	Animal Scientific Procedures Act 1986
BSA	Bovine serum albumin
CKD	Chronic kidney disease
DAPI	4',6-diamidino-2-phenylindole
ECM	Extracellular matrix
EDTA	Ethylenediaminetetraacetic acid
IgG	Immunoglobulin G
mAbs	Monoclonal antibodies
PBS	Phosphate buffered saline
TE	Target engagement
TG	Transglutaminase
TGF-β	Transforming growth factor-β
TO	Target occupancy
UK	United Kingdom
UUO	Unilateral ureteral obstruction

Supplementary Information

The online version contains supplementary material available at <https://doi.org/10.1186/s12882-025-04467-8>.

Supplementary Material 1: Figure S1 Sequence alignment between human and cynomolgus monkey TG2 protein. Sequence alignment demonstrates that zampilimab, DH2 and IA12 are 100% conserved between human and cynomolgus monkey TG2.

Acknowledgements

The authors would like to thank the healthy volunteers for their support with the human skin biopsy study. The authors would like to acknowledge Radhika Bhatia, PhD, of UCB, for publication and editorial support. Medical writing support for the development of this manuscript, under the direction of the authors, was provided by Sarah Hibbert, PhD, and Jo Badawy, BSc, of Ashfield MedComms, Macclesfield, UK, an Inizio company, and funded by UCB, in

accordance with Good Publication Practice (GPP 2022) guidelines (<https://www.ismpp.org/gpp-2022>).

Author contributions

GO and LH were involved in the design and execution of the preclinical studies. GO, LH, GJJ, and RB were involved in the design and execution of the human skin biopsy study. AB was involved in the image analysis of both preclinical and human skin biopsy studies. GO was principal investigator for the human skin biopsy study and co-ordinated skin sampling. LH was involved in writing the manuscript, developed, optimized, and ran the TG2 TO assay in cynomolgus monkey tissue and part of the human skin biopsies, as well as collating and analyzing the data. GJJ was involved in the experimental design and analysis of the human skin study biopsies. RB was involved in writing the manuscript, further optimization of the TO assay on human skin, running, and analysis of human skin biopsy samples and key input into optimization of analysis algorithms developed by OracleBio. AB developed and performed all the analyses at OracleBio. TS contributed to the concept and design of the work. TSJ developed the concept of the assay, the study design, and helped to write the manuscript.

Funding

These studies were funded by UCB.

Data availability

The datasets generated and/or analyzed during the studies are not publicly available as data from non-clinical studies are outside of UCB's data sharing policy but are available from the corresponding author on reasonable request.

Declarations

Ethics approval and consent to participate

Ownership of the animals used in this study resided with Prisms Biotechnologies (Shanghai, China), who also undertook the animal work, which was approved by the Institutional Animal Care and Use Committee under study number 2015-PS11-002 (license code No. 204 0000037). UCB representatives (including an animal care and welfare officer) assessed facilities and procedures prior to the study start to ensure best practice animal welfare in accordance with United Kingdom (UK) Home Office guidelines and the Animal Scientific Procedures Act 1986 (ASPL). A UCB representative was present during all animal experiments to ensure compliance with ASPL. The study is reported in accordance with the ARRIVE guidelines. The human skin biopsy study was a research collaboration with the University of Oxford and was approved by the South Central - Oxford B Research Ethics Committee (reference 16/SC/0457), in accordance with the Declaration of Helsinki. All participants provided informed consent.

Consent for publication

Not applicable.

Competing interests

RB is an employee of UCB who in-licensed zampilimab and holds/has access to stock options. LH, TS, GJJ, and TSJ were employees of UCB at the time the work was completed and held/had access to stock options during this time. TSJ is an inventor on patent WO2013/175229 A1 (Anti-transglutaminase 2 antibodies) relating to the discovery and humanization of zampilimab. AB was an employee of OracleBio at the time the study was conducted. AR was an employee of Veramed at the time the study was conducted. GO is supported by the UK Medical Research Council and was in receipt of UCB research funding administered through the University of Oxford.

Author details

¹UCB, Slough, UK

²OracleBio, Biocity, Scotland, UK

³MRC Human Immunology Unit, University of Oxford, Oxford, UK

⁴Present address: Mestag Therapeutics Ltd, Cambridge, UK

⁵Present address: Senisca Ltd, Exeter, UK

References

1. Grimwood S, Hartig PR. Target site occupancy: emerging generalizations from clinical and preclinical studies. *Pharmacol Ther.* 2009;122(3):281–301.
2. Stefaniak J, Huber KVM. Importance of quantifying drug-target engagement in cells. *ACS Med Chem Lett.* 2020;11(4):403–6.
3. Pentz RD, Harvey RD, White M, Farmer ZL, Dashevskaya O, Chen Z, et al. Research biopsies in phase I studies: views and perspectives of participants and investigators. *IRB.* 2012;34(2):1–8.
4. Hartung EA. Biomarkers and surrogate endpoints in kidney disease. *Pediatr Nephrol.* 2016;31(3):381–91.
5. Eckert RL, Kaartinen MT, Nurminskaya M, Belkin AM, Colak G, Johnson GV, Mehta K. Transglutaminase regulation of cell function. *Physiol Rev.* 2014;94(2):383–417.
6. Huang L, Haylor JL, Hau Z, Jones RA, Vickers ME, Wagner B, et al. Transglutaminase Inhibition ameliorates experimental diabetic nephropathy. *Kidney Int.* 2009;76(4):383–94.
7. Tatsukawa H, Hitomi K. Role of transglutaminase 2 in cell death, survival, and fibrosis. *Cells.* 2021;10(7):1842.
8. Belkin AM. Extracellular TG2: emerging functions and regulation. *FEBS J.* 2011;278(24):4704–16.
9. Wang Z, Griffin M. TG2, a novel extracellular protein with multiple functions. *Amino Acids.* 2012;42(2–3):939–49.
10. Johnson TS, Skill NJ, El Nahas AM, Oldroyd SD, Thomas GL, Douthwaite JA, et al. Transglutaminase transcription and antigen translocation in experimental renal scarring. *J Am Soc Nephrol.* 1999;10(10):2146–57.
11. Wang Z, Stuckey DJ, Murdoch CE, Camelliti P, Lip GYH, Griffin M. Cardiac fibrosis can be attenuated by blocking the activity of transglutaminase 2 using a selective small-molecule inhibitor. *Cell Death Dis.* 2018;9(6):613.
12. Johnson TS, El-Koraie AF, Skill NJ, Baddour NM, El Nahas AM, Njlooma M, et al. Tissue transglutaminase and the progression of human renal scarring. *J Am Soc Nephrol.* 2003;14(8):2052–62.
13. Grenard P, Bresson-Hadni S, El Alaoui S, Chevallier M, Vuitton DA, Ricard-Blum S. Transglutaminase-mediated cross-linking is involved in the stabilization of extracellular matrix in human liver fibrosis. *J Hepatol.* 2001;35(3):367–75.
14. Olsen KC, Sapinoro RE, Kottmann RM, Kulkarni AA, Iismaa SE, Johnson GV, et al. Transglutaminase 2 and its role in pulmonary fibrosis. *Am J Respir Crit Care Med.* 2011;184(6):699–707.
15. Griffin M, Smith LL, Wynne J. Changes in transglutaminase activity in an experimental model of pulmonary fibrosis induced by Paraquat. *Br J Exp Pathol.* 1979;60(6):653–61.
16. Fisher M, Jones RA, Huang L, Haylor JL, El Nahas M, Griffin M, Johnson TS. Modulation of tissue transglutaminase in tubular epithelial cells alters extracellular matrix levels: a potential mechanism of tissue scarring. *Matrix Biol.* 2009;28(1):20–31.
17. Huang L, Haylor JL, Fisher M, Hau Z, El Nahas AM, Griffin M, Johnson TS. Do changes in transglutaminase activity alter latent transforming growth factor beta activation in experimental diabetic nephropathy? *Nephrol Dial Transpl.* 2010;25(12):3897–910.
18. Nunes I, Gleizes PE, Metz CN, Rifkin DB. Latent transforming growth factor-beta binding protein domains involved in activation and transglutaminase-dependent cross-linking of latent transforming growth factor-beta. *J Cell Biol.* 1997;136(5):1151–63.
19. Prat-Duran J, Pinilla E, Nørregaard R, Simonsen U, Buus NH. Transglutaminase 2 as a novel target in chronic kidney disease - Methods, mechanisms and Pharmacological Inhibition. *Pharmacol Ther.* 2021;222:107787.
20. Da Silva Lodge M, Pullen N, Pereira M, Johnson TS. Urinary levels of pro-fibrotic transglutaminase 2 (TG2) May help predict progression of chronic kidney disease. *PLoS ONE.* 2022;17(1):e0262104.
21. Johnson TS, Fisher M, Haylor JL, Hau Z, Skill NJ, Jones R, et al. Transglutaminase Inhibition reduces fibrosis and preserves function in experimental chronic kidney disease. *J Am Soc Nephrol.* 2007;18(12):3078–88.
22. Shweke N, Boulos N, Jouanneau C, Vandermeersch S, Melino G, Dussaule JC, et al. Tissue transglutaminase contributes to interstitial renal fibrosis by favoring accumulation of fibrillar collagen through TGF-beta activation and cell infiltration. *Am J Pathol.* 2008;173(3):631–42.
23. Oh K, Park HB, Byoun OJ, Shin DM, Jeong EM, Kim YW, et al. Epithelial transglutaminase 2 is needed for T cell interleukin-17 production and subsequent pulmonary inflammation and fibrosis in bleomycin-treated mice. *J Exp Med.* 2011;208(8):1707–19.
24. Maamra M, Benayad OM, Matthews D, Kettleborough C, Atkinson J, Cain K, et al. Transglutaminase 2: development of therapeutic antibodies reveals four

Received: 22 April 2024 / Accepted: 8 September 2025

Published online: 21 November 2025

- inhibitory epitopes and confirms extracellular function in fibrotic remodeling. *Br J Pharmacol.* 2022;179(11):2697–712.
25. Haroon ZA, Hettasch JM, Lai TS, Dewhirst MW, Greenberg CS. Tissue transglutaminase is expressed, active, and directly involved in rat dermal wound healing and angiogenesis. *FASEB J.* 1999;13(13):1787–95.
 26. Bowness JM, Tarr AH, Wong T. Increased transglutaminase activity during skin wound healing in rats. *Biochim Biophys Acta.* 1988;967(2):234–40.
 27. Huang L, Bon H, Maamra M, Holmes T, Atkinson J, Cain K, et al. The effect of TG2-inhibitory monoclonal antibody zampilimab on tissue fibrosis in human in vitro and primate in vivo models of chronic kidney disease. *PLoS ONE.* 2024;19(5):e0298864.
 28. Huang L, Ni J, Duncan T, Song Z, Johnson TS. Development of a unilateral ureteral obstruction model in cynomolgus monkeys. *Anim Model Exp Med.* 2021;4(4):359–68.
 29. Sugimura Y, Hosono M, Wada F, Yoshimura T, Maki M, Hitomi K. Screening for the preferred substrate sequence of transglutaminase using a phage-displayed peptide library: identification of peptide substrates for TGASE 2 and factor XIIIa. *J Biol Chem.* 2006;281(26):17699–706.

Publisher's note

Springer Nature remains neutral with regard to jurisdictional claims in published maps and institutional affiliations.